APPLICATION OF BROMOANTHRACENE BASED ORGANIC DYES AS DYE SENSITIZED SOLAR CELLS - MOLECULAR MODELLING APPROACH

[1]T.Saravana Kumaran, [2]I.Ragavan, [3]A.Prakasam and [4]P.M.Anbarasan
[1]Research scholar, Department of Physics, Thiruvalluvar Government Arts College, Rasipuram, Tamilnadu, India, Pin-637401
[2]Research scholar, Nano and Hybrid Materials Laboratory,Department of Physics, Periyar University, Salem 636 011, Tamilnadu, India.
[3]Assistant Professor, Department of Physics, Thiruvalluvar Government Arts College, Rasipuram, Tamilnadu, India, Pin-637401
[4]Professor, Nano and Hybrid Materials Laboratory,Department of Physics, Periyar University, Salem 636 011, Tamilnadu, India.

Abstract

Thestructure of molecule was based on Donor-π bridge-Acceptor. From this the different type of donor are investigated. This work based on Hartree-Fock (HF) and Density functional theory (DFT), the present study analyses the molecular and electronic structures, polarizabilities and hyperpolarizabilities of organic dye sensitizer of Bromoanthracene. Ultraviote. Thestructure of molecule was based on Donor-π bridge-Acceptor. From this the different type of donor are investigated. This work based on Hartree-Fock (HF) and Density functional theory (DFT), the present study analyses the molecular and electronic structures, polarizabilities and hyperpolarizabilities of organic dye sensitizer of Bromoanthracene. Ultraviolet-visible (UV-Vis) spectrum were analysed using Time Dependent-Density Functional Theory (TD-DFT). The theoretical results have demonstrated that TDDFT calculations using the polarizable continuum model (PCM) were logically capable of predicting the excitation energies, the absorption and the emission spectra of the molecules. The prominent features of the electronic absorption spectrum in the visible and near-infrared regions were designated based upon TDDFT calculations. The bands of absorption are assigned to n $\rightarrow\pi^*$ transitions. The chemical hardness (η), ionization potential (IP), electron affinity (EA), dipole moment (μ), absolute electronegativity (χ) and electrophilicity index (ω) are also measured to find the stability of the molecules.

Keywords: Dye-sensitized solar cells, Density functional theory, Time Dependent-Density Functional Theory, Dye sensitizer, Electronic and Absorption spectrum.

1. Introduction

Among the metal free organic dyes D- π -A structure molecules are proposed a strong candidates because of their geometry, electronic structure, UV-visible region, light harvesting efficiency, NLO property and global reactivity are excellent. In this work our molecule also based on D- π -A structure. The D- π -A structure consist of Bromoanthracene as π-bridge molecule, amide and methyl group are acts as a donors. Some properties of this molecules are given below. In the field of dye sensitized solar cell, Bromoanthracene is certainly one of the most extensively investigated organic compounds. The essential role in the investigation of photo induced isomerizations is one of the reasonableness for the continuing interest in this molecule. These processes are not only crucial for the understanding of many photochemical transformations and their solvent dependence but also for our own view of the external world, as they form a key step in the visual process. Bromoanthracene compounds are indeed frequently textbook examples of photochemical isomerization. Their reactivity has a significant role as model compound of biological phototropic systems. They also serve as building blocks for organic materials, whose properties could be used in optical and electro-optical implementations such as optical data storage, laser dyes, nonlinear optics, or photo chemically, cross-linked polymers. Significant interest occurs in the form and reinforcement of materials manifesting large second-order

nonlinear optical response [1-3] by cause of the potential applications in telecommunications, optical computing, and optical signal processing [1, 3-9]. These implementations require thermally implied materials with high nonlinear optical (NLO) response. Depending on the particular application, the use of organic materials may offer significant benefits over conventional inorganic crystals. In the past decade, considerable effort emphasised on the development of organic materials with large molecular hyper polarizabilities, enriched optical transparency, and good thermal stability. The elevated singlet state properties of Trans form is governed by fluorescence from the S1 state. This occurrence of photochromism namely, Bromoanthracene photo-isomerization can be easily observed by a single steady-state fluorescence technique. An essential stage in the olefinic photo-isomerization process, in the singlet or triplet excited state, implies twisting of Anthracene fragments relative to one another. Symmetric Bromoanthracene derivatives are commonly, thermally and chemically stable, and possess immerssion and fluorescence properties that are convenient for examining by coherent optical proficiencies [10-19]. Symmetric Bromoanthracene are applied in the manufacture of organic dichroic dyes, thin optical polarizers, electronic microscopes, image stabilizers and other optoelectronic devices. They play an increasingly vital role in the area of photophysical, photochemical, biophysical and technical investigations [20-29]. Bromoanthracene's symmetric derivatives are of great interest in terms of their electronic structure and geometry of the ground and excited state [29].

Amide derivatives are well-known as a superior properties and has been used due to its thermal stability, chemical resistance, and mechanical properties. [30] Since polyamide was developed as an aerospace polymer by NASA in the 1970s, it has been applied to various industries [31, 32] and has been extensively studied. The utilization of Amide derivatives are actively used in electronic materials, similarly semiconductors and integrated circuits, for the continued development of the IT industry. However, an Amide derivative has a immensely combined aromatic structure and a high glass transition temperature; therefore, it shows high residual stress and poor workability. [33]. recently, the detailed binding mechanisms to saturated and unsaturated light hydrocarbons has been rationalised in a hydroxyl-functionalised Metal Organic Frame work [34]. Within the field of carbon capture, materials functionalised with amines ($-NH_2$), imines (-NH), and amides (-CONH) dominate, largely due to their potential to form specific interactions with CO_2, leading to highly selective CO_2 uptakes. Although high CO_2 consumption has been examined in a number of amine-, imine-, and amide-functionalised Metal Organic Frame work,[35] molecular insight into the direct binding between adsorbed CO_2 molecules and porous host (especially towards these functional groups) is overall inadequacy. Lately, direct $H_2N(\delta-)\cdots(\delta+)CO_2$ binding has been observed in a Zn(II) Metal Organic Frame work incorporating amine groups that protrude into the pore, providing structural insight into the observed high CO_2 adsorption in this material [36]. The incorporation of pendent amide (-CONH-) and/or amine groups into Metal Organic Frame work is thus regarded generally as a promising approach to enhance CO_2 uptake because of the formation of hydrogen bonds with amides serving as both hydrogen bond acceptors (*via* C=O) and donors (*via* N-H). A sequence of amide functionalised MOFs have been synthesised and demonstrated to exhibit high CO_2 uptakes and selectivities [35,37] Likewise, computational studies attribute this to the specific binding and formation of hydrogen bonds between adsorbed CO_2 molecules and free amide or amine groups as a result of enhancing adsorption affinity and selectivity for CO_2 [35c,37c,38]. However, to date there is a few physical investigations on the precise role of amides in CO_2 binding in Metal Organic Frame work. Besides, the challenge of such investigations is increased in Metal Organic Frame work systems insisting open metal sites owing to the inevitable competition for guest binding between the open metal sites and the organic functional group(s) in the pore. Here, the synthesis of the report, structure and gas adsorption properties of an amide functionalised pyrimidyl Cu(II)-carboxylate Metal Organic Frame work, MFM-136, which shows a high CO_2 adsorption capacity (12.6 mol /g at 20 bar and 298 K).

Fluorine plays a conspicuous and increasingly essential role within pharmaceuticals and agrochemicals, together in materials science, because one or a few fluorine atoms substituted at specific sites in organic compounds can severely alter their chemical and biological properties, such as solubility, metabolic and oxidative stability, lipophilicity, and bioavailability. Further, Tsuzuki and his co-workers investigated F- and CF_3-substituted oligomers and examined the electron mobility to be up to 0.55 cm^2/ V sec, considering the

single crystal transistors exhibited high electron mobilities up to 3.1 cm^2/ Vsec. In furtherance of achieving high air stability and developing a high performance n-type organic semiconductors, a series of oligomers containing -$CF_3$and -CNgroups were synthesized by Shoji *et al.* Besides, Yu and co-workers also experimentally developed two air stable n-type CF_3-triphenodioxazines. The present paper has investigated the influence of trifluromethyl (- CF_3) on the charge transport properties of napthalene.

A methyl derivative endeavours the advantages of good solubility in organic solvents, high electron mobility and high electron affinity. Methyl derivatives has also become the most important and broadly utilized as electron acceptor or electron donors in solar cells. Solar Cells based on methyl derivatives demonstrate 3–5% power conversion efficiency (PCE) under an illumination of AM 1.5G [39, 40]. However, a methyl derivative illustrates disadvantages such as weak absorption in the visible region and a low level energy at the lowest unoccupied molecular orbital (LUMO). Weak absorption in the visible region combines the contribution of methyl derivatives to illuminate harvesting in photovoltaic conversion. Ten years ago, numerous methyl derivatives analogues with modified substitution groups have been reviewed as electron acceptors [41–45]. After all, most of these analogues exhibit poor photovoltaic performance [41–45]. In order to improve the PCE of Solar Cells, considerable research has been devoted to analyse a new acceptor material with a broader absorption spectrum, higher LUMO energy level and electron mobility, and an appropriate electron energy level than those of existing materials. One of the adequacy means of modifying fullerene derivatives via bi-addition or multi-addition is to increase the LUMO level of fullerene derivative electron acceptors; further, many fullerene bis-adducts and multi-adducts with high LUMO energy levels have been developed as acceptors in Solar Cells [46–65].

2. Computational Details

The density functional theory (DFT) was used to acquire the minimum energy molecular structure (geometry optimization), chemical reactivity, and the highest occupied molecular orbital (HOMO) and lowest unoccupied molecular orbital (LUMO) energy levels. The parameters of calculated chemical reactivity were obtained using the formulae reported by Parr and Pearson [66] and Gázquez et al. [67] using the ionic and neutral states energy values. The above calculations were obtained by the B3LYP density functional theory [68] and the 6-311++G (d, p) basis set [69-70]. The energy of the vertical excitation, the oscillator strength and the transitions all corresponding to the UV–Vis absorption spectra were obtained with time-dependent DFT (TD-DFT), using the B3LYP time dependent density functional theory [68] with the above-mentioned basis set. The non-equilibrium calculation protocol [71-72] was used for obtaining the UV–Vis spectrum; meanwhile, the considerations for the effect of the solvent (aniline) were through integral equation formalism polarizable continuum model (PCM) [73]. The UV–Vis spectrum graphics, the oscillator strength and the electronic transitions were processed [74-75] using the Gaussian model. All calculations were implemented with Gaussian 09 Revision D.01 [76].

3. Results and Discussion

3.1 Molecular Structure

The optimized molecular structure of the dyes BTA1, BTA2 and BTA3 determined by B3LYP/6-311++G (d, p) are shown in Figure 1.Some selected bond length, bond angle and dihedral angle are listed in the Table 1. In all the dyes most of the bond length, bond angle and dihedral angle are same only some different value is found.

Table 1. The selected bond length (angstrom), bond angle (degree) and dihedral angle (degree) of the dyes BTA1, BTA2 and BTA3.

Dye	Atoms	Value
BTA1	C11-H26	1.0863
	C6-C5-C10	123.5833
	C7-C8-C11-C12	179.985

BTA2	C5-C10	1.4071
	C5-C10-Br15	118.4809
	C8-C9-C14-H29	180.0139
BTA3	C11-H24	1.0867
	H27-C16-H29	107.8901
	C8-C11-C12-C16	179.994

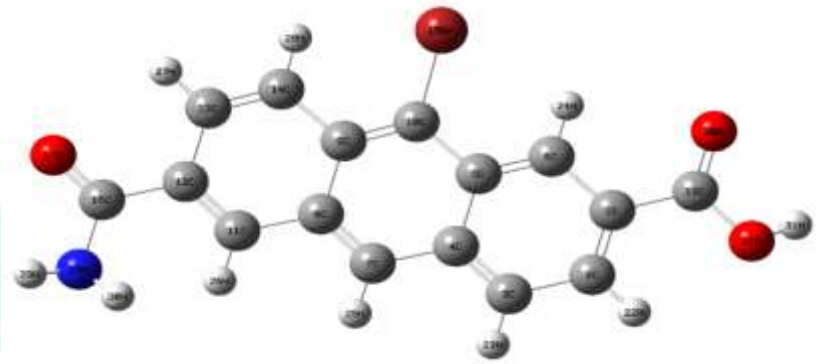

BTA 1

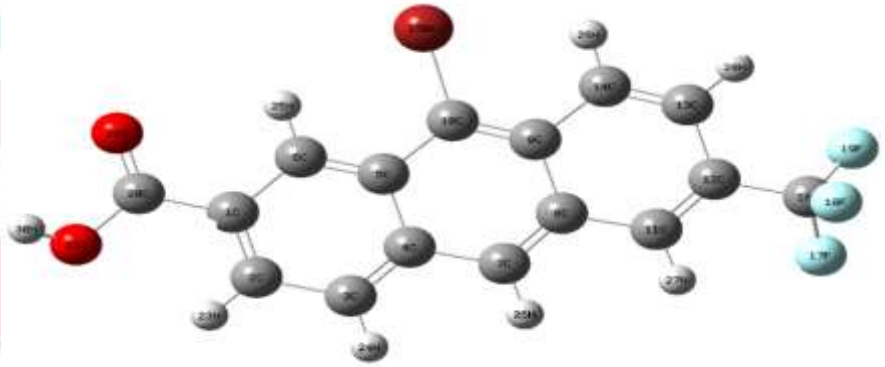

BTA 2

BTA 3

Figure 1. The optimized molecular structure of the dyes D1, D2 and D3

3.2 Electronic Structure

It is very important to determine the distribution pattern of the frontier molecular orbitals (FMO) because it provides the charge distribution of the atoms. The highest occupied molecular orbitals (HOMOs) and the lowest unoccupied molecular orbitals (LUMOs) of the dye BTA1, BTA2 and BTA3 obtained at the optimised electronic structure using B3LYP/6-311++G (d, p) are demonstrated in Figure 2.

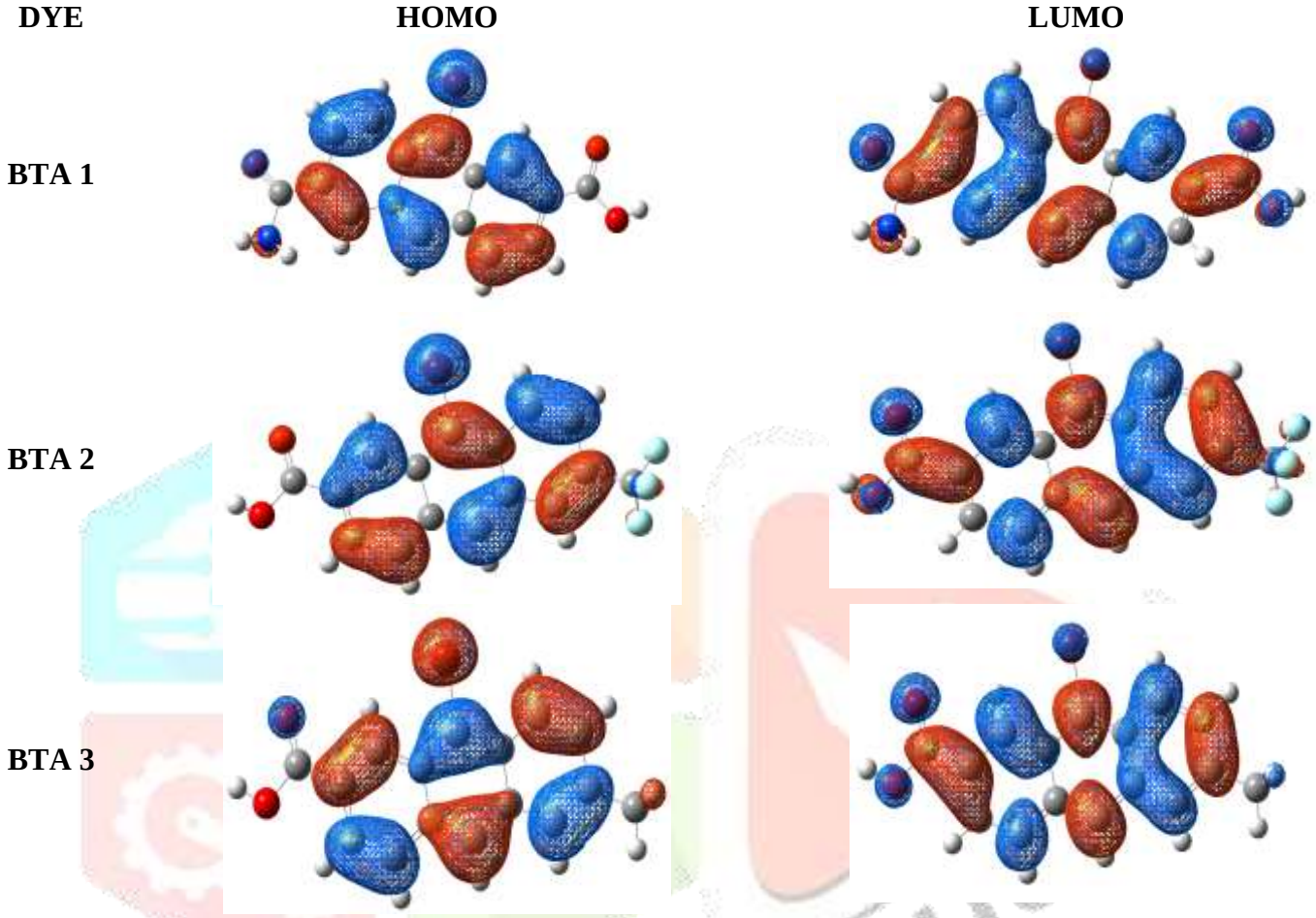

Figure 2. Electronic structure of the dyes BTA 1, BTA 2 and BTA 3.

To create an adequate charge-separated state by photo absorption, it is prepared that the HOMO is localised on donor and the LUMO on the acceptor. Then the dyes BTA1, BTA2 and BTA3 are based on D- π -A structure. From the structure the HOMOs are mainly present in donor and π-bridge region and the LUMO are present in acceptor regions. From the figure it is clearly pointed that the charge-separated state is created by the transition from HOMO to LUMO; in these dyes, the HOMO–LUMO excitation can be assign to intramolecular charge-transfer transition from donor to acceptor. The electron density in frontier molecular orbital is imbricate between the HOMO and LUMO, it submit that good induction and electron- withdrawing properties for the donor and acceptor [77]. Therefore, one could conclude that strong overlap between donor and acceptor, it subsequently toward conduction band of TiO_2.

The diagram of energy level HOMO and LUMO molecular orbitals of the dyes BTA1, BTA2 and BTA3 are shown in Figure 3. The LUMO level was distinguished with the conduction band of the anatase phase of TiO_2 because it is considered the most sufficient phase for photovoltaic applications, and the measurements have shown that the lifetimes of photoexcited carriers are longer in anatase [78]; according to experimental results, it has considered a conduction band of TiO_2 at −4.0 eV versus the vacuum level (this value is commonly accepted in the DSSC literature) [79-82]. The HOMO level is compared with the redox potential of an electrolyte; I^-/I_3^- has agreeable penetration ability into the porous semiconductor film, fast dye regeneration and relatively slow

recombination with injected photoelectrons. Moreover, I^-/I_3^- is the only redox couple which has been analysed to have long-term stability [83].

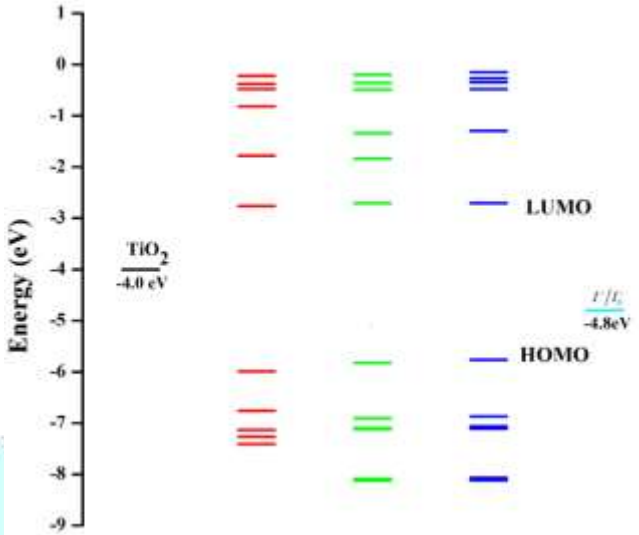

Figure 3. The energy level diagram of the dyes BTA, BTA2 and BTA3

.

All the molecules fulfil the energy levels required for their potential use as photo sensitizers; viz, the LUMO level is above the conduction band of the metallic oxide TiO_2, which allows the charge transference from the dye to the semiconductor, the level of HOMO is below the redox potential of the electrolyte I^-/I_3^- (−4.8 eV) [84] which allows the regeneration of the dye [85]. In this study, all the molecules have quite parallel energy levels and as a result one cannot determine which one will present a better electron transfer to the oxide. However, we can remark that the BTA1 dye are the closest to the TiO_2 conduction band with a LUMO of −2.76 eV.

3.3 HOMO LUMO Band Gap

The HOMO LUMO energy gap were calculating using B3LYP/6-311++G (d, p) and CAM B3LYP/6-311++G (d, p) and the calculated results are outline in the Table 2. The HOMO-LUMO was studied and the values decrease from 3.23eV to 3.06 eV for the dyes BTA1 to BTA3. The study also examined this HOMO-LUMO gap in CAM B3LYP, then the values of band gap decrease from 5.72eV to 5.54eV. The HOMO-LUMO gap decreases as a few donor increases. However replacing the methyl group instead the amide group the band gap decrease from 3.23eV to 3.06 eV. From changing the donor we get the band gap difference is 0.17eV.

Table 2. The HOMO and LUMO energy in eV obtained in B3LYP/6-311++G (d, p) and CAM B3LYP/6-311++G (d, p)

Dye	B3LYP			CAM/ B3LYP		
	HOMO (eV)	LUMO (eV)	HOMO-LUMO (eV)	HOMO (eV)	LUMO (eV)	HOMO-LUMO (eV)
BTA1	5.92	2.65	3.27	6.14	1.57	4.57
BTA2	6.15	2.80	3.35	6.16	1.49	4.67
BTA3	5.64	2.31	3.37	6.80	1.22	5.58

3.4 UV-Visible Absorption Spectra

The electronic absorption spectra of the dyes BTA1, BTA2 and BTA3 are evaluated in vacuum and aniline solvent were performed using TD-DFT/B3LYP/6-311+G (d, p) and the calculated results are shown in the Figure 4. It is observed that the visible region in the absorption is on the UV region for the dyes BTA1, BTA2 and BTA3. For all the three dyes the results of TD-DFT have an ample red shift in vacuum and solvent (aniline).

The distinctness between the vacuum and solvent effects in TD-DFT calculations may result from two senses. The first sense is smaller gap of materials which produce smaller excited energies. Another one is solvent effects. Empirical measurements of electronic absorptions are consistently calculated in solution. Specifically polar solvent, could affect the geometry and electronic structure as well as the molecules' properties through the long-range interaction between Solute molecule and solvent molecule. For this motive, the TD-DFT calculation is harder to make consistent with quantitatively, so TD-DFT calculation with polar solvent calculated. Though the difference exists, the TD-DFT calculations are capable of explain the spectral features of the dye BTA1, BTA2 and BTA3, because of the acceptance of line shape and relative strength as distinguished with the vacuum and solvent.[86]. From the figure 4.4, the absorption spectral regions of dyes BTA1, BTA2 and BTA3 were located at 432 nm, 447 nm and 455 nm respectively. The molecular orbital analysis demonstrated that the dominant absorption bands of all the three dyes were in the region n→π* transition.

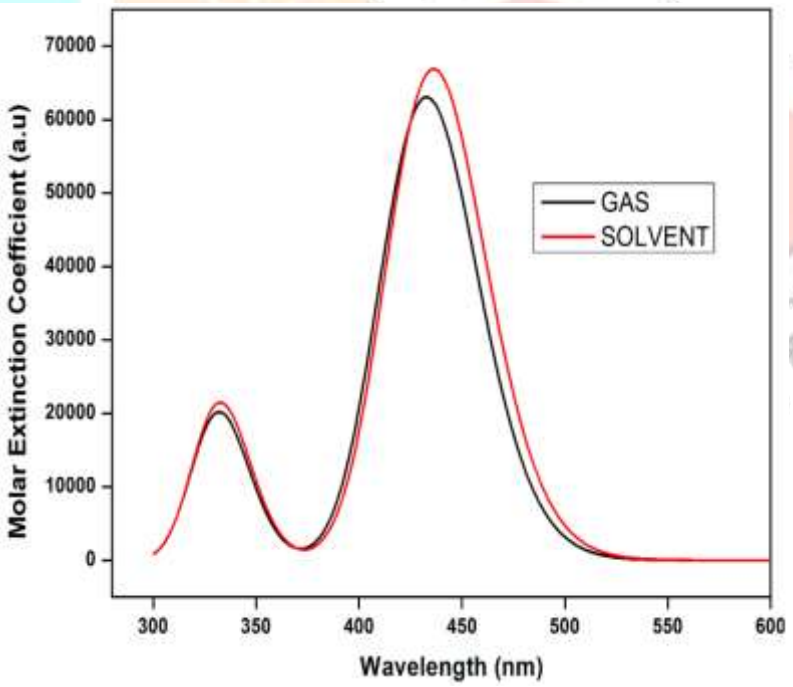

BTA1.

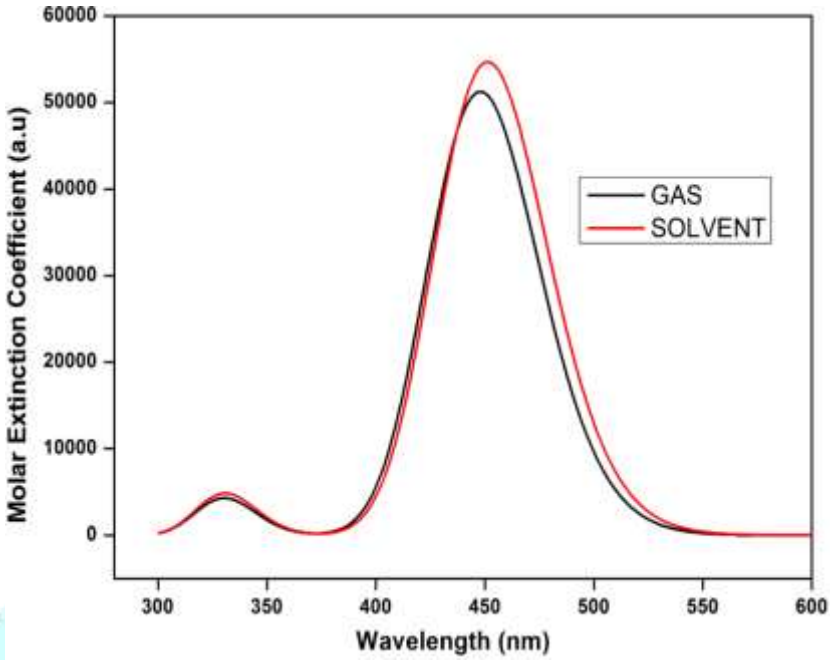

BTA2.

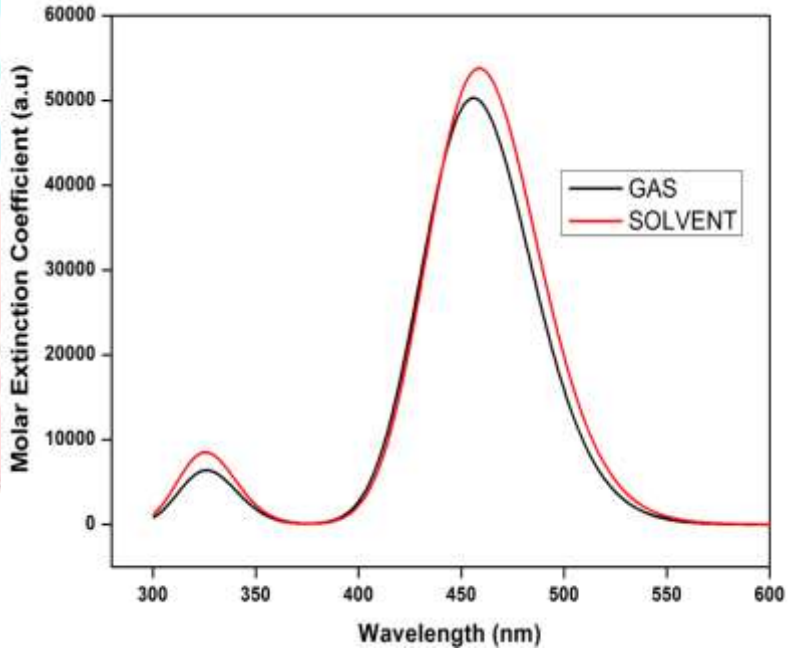

BTA 3

Figure 4. The electronic absorption spectra of the dyes BTA 1, BTA 2, BTA 3.

3.5 Light Harvesting Efficiency

Generally, efficiency of the DSSCs depends on the photosensitizers. Photosensitizers are categorizing into two types. They are metal complex and metal-free organic sensitizers. The basic structural substance of metal-free dyes is donor-pi-spacer-acceptor (D- π -A). The photovoltaic properties of such dyes can be adjusted by selecting perfect groups within the D-π-A structure. Therefore, TD-DFT is used in this study which is a successful tool for finding the ground and agitated state properties of photo sensitizer aggregates as related to other high level quantum approaches because it determine the orbitals are perfect for the typical MO-theoretical survey and interpretations.

The structural modifications which enhance the electron injection efficiency of Bromoanthracene based DSSCs are explained. Of course, all conversions are theoretically realizable and a large panel of new structure can be analysed. The light harvesting efficiency (LHE) of the dye sensitizer should be as large as possible to maximize the photocurrent reaction and can be calculated by the following equation

$$LHE = 1\text{-}10^{-f} \quad (1)$$

Where f is the oscillator strength of the dye with the corresponding wavelength associated to the peak absorbance through intramolecular charge transfer. The LHE is the efficiency of dye in responding to light which point out the efficiency of DSSC also. All values of the calculated LHE are collected in Table 3. It is also examined that exchange of acceptor and donor atoms can enrich the properties of Bromoanthracene and these derivatives can be used in DSSC.

Table 3. Absorption wavelength (in nm), oscillator strength (f in a.u.), orbital transitions and light harvesting efficiency (LHE) of the dyes BTA1, BTA2 and BTA3.

Dye	Wavelength(nm)	F	LHE	Major Contributions
BTA1	437	0.1085	0.221	H->L (98%)
	347	0.0455	0.099	H-1->L (18%), H->L+1 (79%)
	325	0.0038	0.008	H-2->L (82%), H-2->L+2 (10%)
BTA2	423	0.1033	0.211	H->L (98%)
	347	0.0718	0.152	H-1->L (16%), H->L+1 (81%)
	294	0.4186	0.618	H-2->L (31%), H-1->L (58%)
BTA3	430	0.1078	0.2198	H->L (98%)
	359	0.105	0.214	H-1->L (13%), H->L+1 (85%)
	294	0.522	0.699	H-1->L (75%), H->L+1 (14%)

3.6 Overall Efficiency

As known to us, the PCE of DSSC devices is exploited by the short-circuit current density (J_{SC}), the open-circuit photovoltage (V_{OC}), the fill factor (ff), and the intensity of the incident light (P_{IN}), is can be calculated by the following equation [87]

$$\eta = FF\frac{V_{OC}J_{SC}}{P_{IN}} \quad (2)$$

In DSSC, Voc can be calculated by the following equation

$$V_{OC} = \frac{E_{CB}}{q} + \frac{kT}{q}\ln\left(\frac{n_C}{N_{CB}}\right) - \frac{E_{redox}}{q} \quad (3)$$

Where the open-circuit photo voltage V_{oc} is calculated by the energy distinctness between the semiconductor E_{CB} and the electrolyte redox potential. Usually, the solution I^-/I_3^- is used as the electrolyte, so one may take it as a constant. ΔCB is the main influent factor of V_{oc}, which can be articulated as follows: [88]

$$\Delta CB = -\frac{q\mu_{normal}\gamma}{\varepsilon_0\varepsilon} \quad (4)$$

Where q is the elementary charge, γ is the molecular surface concentration, μ_{normal} is the dipole moment of individual molecular perpendicular to the interface of the semiconductor, and ε_0, ε as constant. It is obvious that a large μ_{normal} will lead to more shift of E_{CB} which will result in larger V_{oc}.

As shown in Table 4, BTA1 is the largest dipole moment, leading to larger V_{oc} which is in outstanding agreement with better efficiency.

Table 4. The Redox potential of the ground state of the dye (E^{dye}), The Redox potential of the excited state of the dye (E^{dye*}), driving force of injection ($\Delta G_{injection}$) and driving force of regeneration (ΔG_{reg}), Calculated Electronic Properties of BTA1, BTA2 and BTA3 dyes

Dye	$\mathbf{E^{dye}}$	$\boldsymbol{\lambda_{max}}$	$\mathbf{E^{dye*}}$	$\boldsymbol{\Delta G_{inject}}$	$\boldsymbol{\Delta G_{reg}}$
BTA1	5.92	437	3.04	-0.96	1.12
BTA2	6.20	423	2.99	-1.01	1.4
BTA3	5.84	430	2.95	-1.05	1.04

The short-circuit current density J_{SC} is calculated by the following equation: [89]

$$J_{SC} = \int_{\lambda} LHE(\lambda)\Phi_{inject}.\eta_{collect}.d\lambda \quad (5)$$

Where LHE (λ) is the light harvesting efficiency at a given wavelength, Φ_{inject} evinces the electron injection adequacy, and $\eta_{collect}$ denotes the charge collection efficiency. For DSSC, the electrode is the same; the only difference is the various sensitizers, so $\eta_{collect}$ can be seen as a consistent [90]. LHE (λ) is mainly determined by the oscillator strength (f) in equation 3.1 [91]. From Table 3, we can know f = 0.87 for BTA1, the oscillator strength of all dyes become smller than BTA1, so does LHE. Φ_{inj} is affiliated to the driving force ΔG_{inject} of electrons injecting from the excited states of dye molecules to the semiconductor substrate. According to the survey [92] when ΔG_{inject}> 0.2 eV, the injection efficiency of electrons (Φ_{inj}) is approximately equal to one. ΔG_{inject} can be approximated as follows: [93]

$$\Delta G_{inject} = E^{dye*} - E_{CB} = E^{dye} + E_{0-0} - E_{CB} \quad (6)$$

Where E^{dye*} is the oxidation potential of the excited dye, E_{CB} is the conduction band edge of the semiconductor (the experimental value −4.0 eV), E_{dye} is the redox potential of the ground state of the dye, and E_{0-0} is the vertical transition energy. Table 4 lists the calculated ground state of the oxidation potential of dyes and their corresponding ΔG_{inject}. From Table 4.4, the absolute values of ΔG_{inject} for BTA1, BTA2 and BTA3 are much greater than 0.4 eV, one can predict that these dyes have adequate driving force for the fast injection of excited electrons. Although ΔG_{inject} of BTA1 and BTA2 is slightly smaller than BTA3. However, too large a ΔG_{inject} may precede energy redundancy, besides resulting in smaller V_{OC} and larger thermalization losses [94, 95]. J_{SC} is also influenced by the regeneration adequacy of the dye (η_{reg}), which is determined by the driving force of regeneration ΔG_{reg}. It can be expressed by the henceforth equation [96]

$$\Delta G_{reg} = E_{redox} - E_{dye} \quad (7)$$

Where E_{redox} is the redox potential −4.8 eV. From the survey of Robson [97], the regeneration process of the dye can significantly influence the efficiency of DSSC. BTA1 having larger driving forces of regeneration, can cause the improvement of η_{reg}, which benefits the increase of short-circuit current density (J_{SC}). Finally, the study finds that BTA1 dye is the better candidates among all the dyes because they perform nicely on the four key parameters (λ_{max}, LHE, J_{SC}, and V_{OC}) and achieve a good balance among these factors. Therefore, BTA1 dye will be promising dyes because of their good conversion efficiency.

3.7 Non-Linear Optical Properties

Further, the static dipole moment (μ), mean polarizability (α_0), polarizability anisotropy (Δα), first order hyperpolarizability (β) and second order hyperpolarizability (γ) for designed dye molecules. The above values were calculated using the formulae as [98, 99]

$$\mu_{tot} = \sqrt{\left(\mu_x^2 + \mu_y^2 + \mu_z^2\right)} \quad (8)$$

$$\alpha_0 = \frac{(\alpha_{xx} + \alpha_{yy} + \alpha_{zz})}{3} \quad (9)$$

$$\Delta\alpha = \left[\left(\alpha_{xx} - \alpha_{yy}\right)^2 + \left(\alpha_{yy} - \alpha_{zz}\right)^2 + \left(\alpha_{zz} - \alpha_{xx}\right)^2\right]^{\frac{1}{2}} \quad (10)$$

$$\beta = \left[\left(\beta_{xxx} + \beta_{xyy} + \beta_{xzz}\right)^2 + \left(\beta_{xxy} + \beta_{yyy} + \beta_{yzz}\right)^2 + \left(\beta_{xxz} + \beta_{zyy} + \beta_{zzz}\right)^2\right]^{1/2} \quad (11)$$

$$\gamma = \frac{1}{6}\left[\left(\gamma_{xxxx} + \gamma_{yyyy} + \gamma_{zzzz}\right) + 2\left(\gamma_{xxxx} + \gamma_{yyyy} + \gamma_{zzzz}\right)\right] \quad (12)$$

Where α_{xx}, α_{yy} and α_{zz} is the polarizability tensor components, $\beta_{xxx}, \beta_{xyy}, \beta_{xzz}, \beta_{xxy}, \beta_{yyy}, \beta_{yzz}, \beta_{xxz}, \beta_{zyy}, \beta_{zzz}$ and $\gamma_{xxxx}, \gamma_{yyyy}, \gamma_{zzzz}$ the first order and second order tensor compounds. The figured dipole moment (μ), mean polarizability (α_0), polarizability anisotropy (Δα), first order hyperpolarizability (β) and second order hyperpolarizability (γ) values were gathered in Table 4.5. From the dyes, BTA1 molecule has large dipole moment at ground and excited state, and then the values are 6.68 and 8.06 Debye respectively. From the dyes, BTA2 molecule has high dipole moment difference between ground and excited state, then the difference has 2.24 Debye. The mean polarizability has 2.35 $x10^{-23}$ e.s.u for the BTA2 dye, it has higher values distinguish to other dyes. The polarizability anisotropy value for BTA1 dye has 6.27 $x10^{-24}$e.s.u, it has higher values compare to other dyes. The static polarizabilities are directly proportional to the dipole moment [100]. From Table 5, it is examined that the dye BTA2 molecule has large dipole moment difference and have high polarizability value of 2.35 $x10^{-23}$ e.s.u.

The first order hyperpolarizability is high for BTA1 molecule compare to the other molecules. The second order hyperpolarizability was determined using the equation (12) and table have shown second order hyperpolarizability results. Among the three dye molecules, high efficient second order hyperpolarizability value obtained in BTA2 dye molecules as 1.95 $x10^{-21}$e.s.u. The BTA3 dye sensitizer show minimum hyperpolarizability value as 1.22 $x10^{-21}$e.s.u. The above results were depending on the donor and functional group substitutions.

A higher values of dipole moment, first and second order hyperpolarizability were essential to active NLO performance. The present results clearly demonstrated that the BTA2 dye molecule particularly can be used in NLO applications.

Table 5. Static dipole moment (μ), mean polarizability (α0), polarizability anisotropy (Δα), First order hyperpolarizability (β) and second order hyperpolarizability (γ) calculated at B3LYP level using 6-31+G(d,p) basis set to the dyes BTA1, BTA2 and BTA3.

Dye	Dipole Moment(μ) in Debye		α_0 ($x10^{-23}$ e.s.u)	Δα ($x\ 10^{-24}$ e.s.u)	β ($x\ 10^{-30}$ e.s.u)	γ ($x\ 10^{-21}$ e.s.u)
	Ground state	Excited state				
BTA1	5.8386	6.8738	1.3001	1.40919	2.2435	5.6135

BTA2	3.1477	3.4960	1.3817	1.61950	2.6062	5.9761
BTA3	4.1562	5.7363	1.1401	1.5697	2.3078	3.9121

3.8 Global and Local Reactivity descriptors

The frontier molecular orbital (HOMO and LUMO) energies, hardness (η), softness (S), ionization potential (IP), energy gap (ΔE), electron affinity (EA), dipole moment (μ), absolute electronegativity (χ) and electrophilicity index (ω) have been calculated by B3LYP/6-311+G are manifested in Table 6.

The HOMO and LUMO energies represent IP and EA respectively in the frame work of Koopmans' theorem

$$IP = -E_{HOMO} \quad (13)$$

$$EA = -E_{LUMO} \quad (14)$$

Table 6. Global and Local Reactivity descriptors of the dyes BTA1, BTA2 and BTA3.

Dye	**IP**	**EA**	**H**	**S**	**χ**	**ω**
BTA1	5.92	2.65	1.86	0.268	4.28	4.935
BTA2	6.15	2.80	1.67	0.299	4.47	5.995
BTA3	5.64	2.31	1.68	0.297	3.97	4.690

The χ and η can determine the following expressions from calculated

$$\chi = \frac{IP + EA}{2} \quad (15)$$

$$\eta = \frac{IP - EA}{2} \quad (16)$$

The S is defined as the inverse of the

$$S = \frac{1}{\eta} \quad (17)$$

The electrophilicity index (ω) formula is

$$\omega = \frac{\mu^2}{2\eta} \quad (18)$$

The high ionization potential indicates high reactivity of atom and molecules. Absolute hardness and softness are to measure the stability and reactivity. A hard molecules having high energy gap correlated to soft molecules [101].

Based upon the foregoing, the study demonstrates the table of chemical hardness (η), electrophilicity (ω), electrodonating power, and electroaccepting power of the dyes. Where as a small difference among the chemical reactivity values are analysed, these allow a deeper study of the electron properties of the dyes. Considering that chemical hardness measures the resistance of the molecule to intermolecular charge transfer [102-103], it is logical to anticipate dyes with the lowest chemical hardness values. Furthermore, the electro accepting power indicates a higher capability to accept charge [104]. From these dyes, the BTA2 molecule has high hardness (η), ionization potential (IP), electron affinity (EA), dipole moment (μ), absolute electronegativity (χ) and electrophilicity index (ω), so dye BTA2 molecule approaches good stability and reactivity compared to other dyes.

4. Conclusion

Theoretical investigation was performed to understand the electronic structure and three bromoanthracene's photo physical properties based D-π-A type organic dyes for DSSC, namely BTA1, BTA2 and BTA3 using the DFT and TD-DFT methods. The computed geometries imply that strong conjugation was formed in the dyes, which is beneficial for the intramolecular charge transfer. The HOMO energies of all these dye were found to approach the redox potential of I^-/I_3^-. Due to their enhanced electron donating abilities and dyes's these LUMO energies these dyes were found to approach the counter electrode TiO_2 due to their enhanced electron accepting abilities. Three dyes in the UV-Visible absorption spectrum were found in their region n→π* transition and all these dyes have smaller red shift found due to their solvent effect. From this dye BTA3 dye has such larger UV-Visible absorption spectral region of 455 nm compared to other two dyes of BTA1 and BTA2. From these dyes, dye BTA1 with an amide donor group was expected to be the best photosensitizer for use in DSSC as it possesses narrow energy gap suitable FMO energy levels, higher LHE and ΔG_{inject} and smallest $\lambda_{max.}$ A DSSC using dye BTA1 may show higher J_{SC} contrasting with other dyes and as a result the overall energy conversion effectiveness could be improved. The dye BTA2 approaches good NLO properties compared to their other dyes. The dye BTA1 approaches good stability and reactivity compared to other dyes.

References

[1.] Prasad, P. N. Williams, D. J. Introduction to Nonlinear Optical Effects in Molecules and Polymers, Wiley: New York, (1991).
[2.] Kanis, D. R. Ratner, M. A. Marks, T. J. Chem. Rev. 94 (1994) 195.
[3.] Dagani, R. Chem. Eng. Ne ws. 74 (1996) 22.
[4.] Lindsay, G.A. K.D. Singer, Polymers for Second-Order Nonlinear Optics; American Chemical Society: Washington, DC, (1995).
[5.] Boyd, D.M. Kuzyk, M.G. Polymers for Electronic and Photonic Applications; cademic Press: New York, (1993).
[6.] Peyghambarian, N. Koch, S.W. A. Mysyrowicz, Introduction to Semiconductor Optics; Prentice Hall: Englewood Cliffs, (1993).
[7.] Kiano, T. Tomaru, S. AdV. Mater. 5 (1993) 172.
[8.] Marder, S.R. Perry, J.W. Science. 263 (1994) 1706.
[9.] Zyss, J. Molecular Nonlinear Optics: Materials, Physics and Devices; Academic Press: Boston, (1993).
[10.] Waldeck, D.H. Chem. Rev. 91 (1991) 415.
[11.] Shahab, S. Filippovich, L. Kumar, R. Darroudi, M. Borzehandani, M.Y. Gomar, M. J. Mol. Struct. 1101 (2015) 109.
[12.] Whitten, D.G. Acc. Chem. Res. 26 (1993) 502.
[13.] Papper, V. Likhtenshtein, G.I. Photochem. J. Photobiol. A Chem. 140 (2001)39.
[14.] Polo, A.S. Itokazu, M.K. Frin, K.M. Patrocinio, A.T. Murakami, I. Neyde, Y. Coord. Chem. Rev. 251 (2007) 255.
[15.] Polo, A.S. Itokazu, M.K. Frin, K.M. Patrocinio, A.T. Murakami, I. Neyde, Y. Coord. Chem. Rev. 250 (2006) 1669.
[16.] Grabowski, R. Rotkiewicz, W. Rettig, W. Chem. Rev. 103 (2003) 3899.
[17.] Momotake, A. Arai, T. J. Photochem. Photobiol. C Photochem. Rev. 5 (2004)
[18.] Brown, T. Holt Jr., H. Lee, M. Heterocycl. Chem. 2 (2006) 1.
[19.] Cai, Y. Luo, Q. Sun, M. Corke, H. Life Sci. 74 (2004) 2157.
[20.] Shahab, S. Agabekov, V. Ariko, N. Filippovich, L. Anisotropy of polarizing polyvinyl alcohol films, in: Advanced Display Technologies: Proc. Of the 15 Intern. Symp, Soc. for Inform. Display, Moscow, Russia, 5 (2006) 163.

[21.] Agabekov, V. Shahab, S. Ariko, N. Filippovich, L. Anisotropy of Polarizing Films with Azodyes. XV Intern. Symp. On Advanced Dis. Tech, SPIE, San Diego, USA, August 27-31, 19/4 (2007) 174.
[22.] Agabekov, V. Ivanova, N. Shahab, S. Kulevskaya, I. Ariko, N. in: Belyaev, V.V. Kompanets I.N. (Eds.), Film Transfect Polarizer. Advanced Display Technologies: Basic Studies of Problems in Inform. Display (FLOWERS 2000), Soc. For Inform. Display, Moscow, Russia. 12 (2000) 141.
[23.] Almodarresiyeh, H.A. Shahab, S.N. Zelenkovsky, V.M. Agabekov, V.E. J. Appl. Spect. 81 (2014) 181.
[24.] Almodarresiyeh, H.A. Shahab, S.N. Zelenkovsky, V.M. Ariko, N.G. Filippovich, L.N. Agabekov, V.E. J. Appl. Spect. 81 (2014) 42.
[25.] Shahab, S. Agabekov, V. Ariko, N. Filippovich, L. Anisotropy of polarizing polyvinyl alcohol films//advanced display technologies, in: Proc. Of the 15 Intern. Symp, Soc. for Inform. Display, Moscow, Russia. 5 (2006) 163.
[26.] Shahab, S. Almodarresiyeh, H.A. Kumar, R. Darroudi, M. J. Mol. Struct. 1088 (2015) 105.
[27.] Shahab, S. Kumar, R. Darroudi, M. Borzehandani, M.Y. J. Mol. Struct. 1083 (2015) 198.
[28.] Almodarresiyeh, H.A. Shahab, S.N. Zelenkovsky, V.M. Agabekov, V.E. J. Appl. Spectr. 81 (2014) 181.
[29.] Becke, A.D. Phys. Rev. A. 38 (1988) 3098.
[30.] Ghosh, M. K. Mittal, K. L. Polyimides: Fundamentals and Applications, Marcel Dekker, New York (1996).
[31.] T. T. Serafi ni, P. Delvigs G. R. Lightsey, J. Appl. Polym. Sci. 16 1972) 905.
[32.] W. Qu , T.-M. Ko , R. H. Vora , T.-S. Chung , Polymer. 42 (2001) 6393 .
[33.] Hsiao, S.H. Chang, L.M. J. Polym. Sci., Part A: Polym. Chem. 38 (2000) 1599.
[34.] Yang, S. Ramirez-Cuesta, A.J. Newby, R. Garcia-Sakai, V. Manuel, P. Callear, S.K. Campbell, S.I. Tang, C.C Schroder, M. Nat. Chem. 7 (2015) 121.
(a) Li, B. Zhang, Z. Li, Y. Yao, K. Zhu, Y. Deng, Z. Yang, F. Zhou, X. Li, G. Wu, H. Nijem, N. Chabal, Y.J. Lai, Z. Han, Y. Shi, Z. Feng, S. Li, J. Angew. Chem. Int. Ed. 51 (2012) 1412.
(b) Du, L. Yang, S. Xu, L. Min, H. Zheng, B. CrystEngComm. 16 (2014) 5520.
(c) Lee, C.H. Huang, H.Y.. Liu, Y.H Luo, T.T. Lee, G.H. Peng, S.M. Jiang, J.C. Chao, I. Lu, K.L. Inorg. Chem. 52 (2013) 3962.
[35.] Vaidhyanathan, R. Iremonger, S.S. Shimizu, G.K.H. Boyd, P.G. Alavi, S. Woo, T.K. Angew. Chem., Int. Ed. 51 (2012) 1826.
[36.] (a) Alsmail, N.H. Suyetin, M. Yan, Y. Cabot, R. Krap, C.P. Lu, J. Easun, T.L. Bichoutskaia, E. Lewis, W. Blake, A.J. Schroder, M. Chem. Eur. J. 20 (2014) 7317.
(b) Zheng, B. Bai, J. Duan, J Wojtas, L. Zaworotko, M.J. J. Am. Chem. Soc. 133 (2011) 748.
(c) Zheng, B. Yang, Z. Bai, J. Li, Y. Li, S. Chem Commun. 48 (2012) 7025.
(d) Xiong, S. He, Y. Krishna, R. Chen, B. Wang, Z. Cryst. Growth Des. 13 (2013) 2670.
(e) Chen, Y.Q. Qu, Y.K. Li, G.R. Zhuang, Z.Z. Chang, Z. Hu, T.L. Xu, J. Bu, X.H Inorg. Chem. 53 (2014) 8842.
(f) Chen, Z. Adil, K. Weselinski, L.J. Belmabkhout, Y. Eddaoudi, M.J. Mater.Chem. A. 3 (2015) 6276.
(g) Lu, Z. Bai, J. Hang, C. Meng, F. Liu, W. Pan, Y. You, X. Chem. Eur. J. 22 (2016) 6277.
[37.] Duan, J. Yang, Z. Bai, J. Zheng, B. Li, Y. Li, S. Chem Commun. 48 (2012) 3058.
[38.] Dennler, G. Scharber, M.C. Brabec, C.J. Adv. Mater. 21 (2009) 1323.
[39.] Ma, W. Yang, C. Gong, X. Lee, K. Heeger, A.J. Adv. Funct. Mater. 15 (2005) 1617.
[40.] Zhao, G. He, Y. Xu, Z. Hou, J. Zhang, M. Min, J. Chen, H.Y. Ye, M. Hong, Z. Yang, Y. Adv. Funct. Mater. 20 (2010) 1480.
[41.] Ross, R.B. Cardona, C.M. Guldi, D.M. Sankaranarayanan, S.G. Reese, M.O. Kopidakis, N. Peet, J. Walker, B. Bazan, G.C. Van Keuren, E. Nat. Mater. 8 (2009) 208.
[42.] Kooistra, F.B. Knol, J. Kastenberg, F. Popescu, L.M. Verhees, W.J. Kroon, J.M. Hummelen, J.C. Org. Lett. 9 (2007) 551.

[43.] Choi, J.H. Son, K.I. Kim, T. Kim, K. Ohkubo, K. Fukuzumi, S. J. Mater. Chem. 20 (2010) 475.
[44.] Yu, Y. Jin, B. Peng, R.F. Fan, L.S. Cai, L.H. Fan, B. Chu, S.J. Synth. Met. 212 (2016) 44.
[45.] He, Y.J. Chen, H.Y. Hou, J.H. Li, Y.F. J. Am. Chem. Soc. 132 (2010) 1377.
[46.] He, Y.J. Peng, B. Zhao, G. Zou, Y. Li, Y. J. Phys. Chem. C 115 (2011) 4340.
[47.] He, Y.J. Zhao, G. Peng, B. Li, Y. Adv. Funct. Mater. 20 (2010) 3383.
[48.] He, Y.J. Chen, H.Y. Zhao, G.J. Hou, J.H. Li, Y.F. Sol. Energy Mater. Sol. Cells 95 (2011) 899.
[49.] He, Y.J. Chen, H.Y. Zhao, G. Hou, J. Li, Y. Sol. Energy Mater. Sol. Cells 95 (2011) 1762.
[50.] Meng, X. Zhang, W. Tan, Z.a. Du, C. Li, C. Bo, Z. Li, Y. Yang, X. Zhen, M. Jiang, F. Chem. Commun. 48 (2012) 425.
[51.] Deng, L.L. Feng, J. Sun, L.C. Wang, S. Xie, S.L. Xie, S.Y. Huang, R.B. Zheng, L.S. Sol. Energy Mater. Sol. Cells. 104 (2012) 113.
[52.] Y. Matsuo, Y. Sato, T. Niinomi, I. Soga, H. Tanaka, E. Nakamura, J. Am. Chem. Soc. 131 (2009) 16048.
[53.] Sakthivel, P. Ban, T.W. Kim, S. Gal, Y.S. Chae, E.A. Shin, W.S. Moon, S.J. Lee, J. C. Jin, S.H. Sol. Energy Mater. Sol. Cells 113 (2013) 13.
[54.] Cheng, Y.J. Liao, M.H. Chang, C.Y. Kao, W.S. Wu, C.E. Hsu, C.S. Chem. Mater. 23 (2011) 4056.
[55.] Chang, C.L. Liang, C.W. Syu, J.J. Wang, L. Leung, M.K. Sol. Energy Mater. Sol. Cells 95 (2011) 2371.
[56.] Yang, T. Jiang, Z. Huang, X. Wei, H. Yuan, J. Yue, W. Li, Y. Ma, W. Org. Electron. 14 (2013) 2184.
[57.] Chi, D. Liu, C. Qu, S. Zhang, Z.G. Li, Y. Li, Y. Wang, J. Wang, Z. Synth. Met. 181 (2013) 117.
[58.] Tian, C.B. Deng, L.L. Zhang, Z.Q. Dai, S.M. Gao, C.L. Xie, S.Y. Huang, R.B. Zheng, L.S. Sol. Energy Mater. Sol. Cells 125 (2014) 198.
[59.] Lenes, M. Wetzelaer, G.J.A. Kooistra, F.B. Veenstra, S.C. Hummelen, J.C. Blom, P.W. Adv. Mater. 20 (2008) 2116.
[60.] Lenes, M. Shelton, S.W. Sieval, A.B. Kronholm, D.F. Hummelen, J.C. Blom, P.W.M. Adv. Funct. Mater. 19 (2009) 3002.
[61.] Voroshazi, E. Vasseur, K. Aernouts, T. Heremans, P. Baumann, A. Deibel, C. Xue, X. Herring, A.J. Athans, A.J. Lada, T.A. Richter, H. Rand, B.P. J. Mater. Chem. 21 (2011) 17345.
[62.] Kim, K.H. Kang, H. Nam, S.Y. Jung, J. Kim, P.S. Cho, C.H. Lee, C.J. Yoon, S.C. Kim, B.J. Chem. Mater. 23 (2011) 5090.
[63.] Zhang, C.Y. Chen, S. Xiao, Z. Zuo, Q.Q. Ding, L.M. Org. Lett. 14 (2012) 1508.
[64.] Ye, G. Chen, S. Xiao, Z. Zuo, Q.Q. Wei, Q. Ding, L.M. J. Mater. Chem. 22 (2012) 22374.
[65.] Parr, R.G. Pearson, R.G. J Am Chem Soc. 105 (1983) 7512.
[66.] Gázquez, J.L. Cedillo, A. Vela, A. J Phys Chem. A.111 (2007) 1966.
[67.] Zhao, Y. Truhlar, D. Theor Chem Acc. 120 (2008) 215.
[68.] Francl, M.M. Pietro, W.J. Hehre, W.J. Binkley, J.S. Gordon, M.S. DeFrees, D.J. Pople, J.A. J Chem Phys. 77 (1982) 3654.
[69.] Rassolov, V.A. Ratner, M.A. Pople, J.A. Redfern, P.C. Curtiss, L.A. J Comput Chem. 22 (2001) 976.
[70.] Cossi, M. Barone, V. J Chem Phys. 115 (2001) 4708.
[71.] Improta, R. Barone, V. Scalmani, G. Frisch, M.J. J Chem Phys. 125 (2006) 054.
[72.] Cancès, E. Mennucci, B. Tomasi, J. J Chem Phys. 107 (1997) 3032.
[73.] Gorelsky, S.I. ALever, .B.P. J. Organomet Chem. 635 (2001) 187.
[74.] Gorelsky, S.I. Wizard software, University of Ottawa, Ottawa, Canada. (2013).
[75.] J. Frisch, G.W. Trucks, H.B. Schlegel, G.E. Scuseria, M.A. Robb, J.R. Cheeseman, H. Nakatsuji, M. Caricato, X. Li, H.P. Hratchian, K. Toyota, R. Fukuda, J. Hasegawa, M. Ishida, R. Nakajima, Y. Honda, O. Kilao, H. Nakai, T. Verven, J.A. Montgomery Jr., J.E. Peralta, F. Ogliaro, M. Bearpark, J.J. Heyd, E. Brothers, K.N. Kudin, V.N. Staroveror,R. Kobayashi, J. Normand, K. Ragavachari, A. Rendell, J.C. Burant, S.J. Tomasi,

M. Cossi, N. Rega, J.M. Millam, M. Klene, J.E. Knox, J.B.Cross, V. Bakken, C. Adamo, J. Jaramillo, R. Gomperts, R.E. Strattmann, O.Yazyev, A.J. Austin, R. Cammi, J.W. Ochetrski, R.L. Martin, K. Morokuma, V.G. Zakrazawski, G.A. Votn, P. Salvador, J.J. Dannenberg, S. Dapprich, A.D. Daniels, O. Farkas, J.B. Foresman, Gaussian O.G., Revision A.O2, Gaussian Inc., Wallingford, CT., 2009.
[76.] Namuangruk, S. Jungsuttiwong, S. Kungwan, N. Promarak, V. Sudyoadsuk, T. Jansang, B. Ehara, M. Theor Chem Acc 14 (2016) 135.
[77.] Xu, M. Gao, Y. Moreno, E.M. Kunst, M. Muhler, M. Wang, Y. Idriss, H. Wöll, C. Phys Rev Lett 106 (2011) 138302.
[78.] Furube, A. Piotrowiak, P. 1st edn. RSC Publishing, New Jersey. (2013).
[79.] Joly, D. Pelleja, L. Narbey, S. Oswald, F. Meyer, T. Kervella, Y. Maldivi, P. Clifford, J.N. Palomares, E. Demadrille, R. Energy Environ Sci. 8 (2015) 2010.
[80.] Nattestad, A. Mozer, A.J. Fischer, M.K.R. Cheng, Y.B. Mishra, A. Bauerle, P. U. Bach, Nat Mater. 9 (2010) 31.
[81.] Pfeifer, V. Erhart, P. Li, S. Rachut, K. Morasch, J. Brötz, J. Reckers, P. Mayer, T. Rühle, S. Zaban, A. Mora Seró, I. Bisquert, J. Jaegermann, W. Klein, A. J Phys Chem Lett. 4 (2013) 4182.
[82.] Cong, J. Yang, X. Kloo, L. Sun, L. Energy Environ Sci. 5 (2012) 9180.
[83.] Cahen, D. Hodes, G. Grätzel, M. Guillemoles, J.F. Riess, I. J Phys Chem. B. 104 (2000) 2053.
[84.] Lu, X. Wei, S. Wu C, M.L. Li, S. Guo, W. J Phys Chem. C. 115 (2011) 3753.
[85.] Anbarasan, P.M. Kumara, P. S. Vasudevana, K. Babub, S. M. Aroulmojic, V. Acta Physica Polonica A Vol. 119 (2011) 3.
[86.] Gratzel, M. Acc. Chem. Res. 42 (2009) 1788.
[87.] Marinado, T. Nonomura, K. Nissfolk, J. Karlsson, M. K. Hagberg, D. P. Sun, L. Mori, S. Hagfeldt, A. Langmuir. 26 (2010) 2592.
[88.] Rühle, S. Greenshtein, M. Chen, S. G. Merson, A. Pizem, H. Sukenik, C. S. Cahen, D. Zaban, A. J. Phys. Chem. B. 109 (2005) 18907.
[89.] Zhang, J. Li, H. B. Sun, Geng, S. L. Y. Wu, Su, Y. Z. M. J. Mater. Chem. 22 (2012) 568.
[90.] Preat, J. Jacquemin, D. Michaux, C. Perpete, E. A. Chem. Phys. 376 (2010) 56.
[91.] Islam, A. Sugihara, H. Arakawa, H. J. Photochem. Photobiol. A.158 (2003) 131.
[92.] Katoh, R. Furube, A. Yoshihara, T. Hara, K. Fujihashi, G. Takano, S. Murata, S. Arakawa, H. Tachiya, M. J. Phys. Chem. B. 108 (2004) 4818.
[93.] Ning, Z. Zhang, Q. Wu, W. Pei, H. Liu, B. Tian, H. J. Org. Chem. 73 (2008) 3791.
[94.] Sayama, K. Tsukagoshi, S. Hara, K. Ohga, Y. Shinpou, A. Abe, Y. Suga, S. Arakawa, H. J. Phys. Chem. B. 106 (2002) 1363.
[95.] Daeneke, T. Mozer, A. J. Uemura, Y. Makuta, S. Fekete, M. Tachibana, Y. Koumura, N. Bach, U. Spiccia, L. J. Am. Chem. Soc. 2012, 134, 16925−16928.
[96.] Robson, K. C. D. Hu, K. Meyer, G. J. Berlinguette, C. P. J. Am. Chem. Soc.135 (2013) 1961.
[97.] Liu, Y. Yang, G. Sun S. and Su, Z. Chin. J. Chem. 30 (2012) 2349.
[98.] S. Jungsuttiwong, R. Tarsang, T. Sudyoadsuk, V. Promarak, P. Khongpracha, S. Namuangruk, Org. Electron. 14 (2013) 711.
[99.] Delgado, M. C. R. Casado, J. Hernandez, V. Navarrete, J. T. L. Orduna, J. Villacampa, B. Alicante, R. Raimundo, J. M. Blanchard P. and Roncali, J. J. Phys. Chem. C. 112 (2008) 3109.
[100.] Balachandran, V. Karpagam, V. Revathi, B. Kavimani, M. Santhi, G. Spectrochim. Acta A. 135 (2015) 1039.
[101.] Parr, R.G. Pearson, R.G. J Am Chem Soc. 105 (1983) 7512.
[102.] J. Martínez Chem Phys Lett. 478 (2009) 310.
[103.] Gázquez, J.L. Cedillo, A. Vela, A. J Phys Chem A. 111 (2007) 1966.